Journal of Solid State Chemistry 184 (2011) 1328–1332

Contents lists available at ScienceDirect

Journal of Solid State Chemistry

journal homepage: www.elsevier.com/locate/jssc

New real ternary and pseudoternary phases in the Li–Au–In system

G.S. Dmytriv [a], V.V. Pavlyuk [a], H. Pauly [b], J. Eckert [c], H. Ehrenberg [c,d,*]

[a] Department of Inorganic Chemistry, Ivan Franko Lviv National University, Kyryla i Mefodia 6, 79005 Lviv, Ukraine
[b] Materials Science, Technische Universität Darmstadt, Petersenstrasse 23, D-64287 Darmstadt, Germany
[c] Institute for Complex Materials, IFW Dresden, Helmholtzstrasse 20, D-01069 Dresden, Germany
[d] Karlsruhe Institute of Technology (KIT), Institute for Applied Materials (IAM), Hermann-von-Helmholtz-Platz 1, D-76344 Eggenstein-Leopoldshafen, Germany

ARTICLE INFO

Article history:
Received 3 February 2010
Received in revised form
27 February 2011
Accepted 8 March 2011
Available online 17 March 2011

Keywords:
Intermetallic compounds
Compound former
Heusler phase
Zintl phase

ABSTRACT

Two real ternary lithium gold indides $LiAu_2In$ and $Li_{280}Au_{22}In_{130}$ ($Li_{0.65}Au_{0.05}In_{0.30}$) were found in the Li–Au–In system. They are isostructural to the respective Ag-alloys. $LiAu_2In$ crystallizes in the $MnCu_2Al$-type structure (*Fm*-3*m*, Heusler phase, $a=6.4982(8)$ Å, based on single crystal XRD-data) and $Li_{280}Au_{22}In_{130}$ in the $Li_{278}Ag_{40}In_{114}$-type structure (*F*-43*m*, $a=19.9970(2)$ Å, based on powder XRD-data). The analogy of the two ternary systems Li–Au–In and Li–Ag–In is additionally reaffirmed by the wide homogeneity range of the pseudoternary solid solution with NaTl-type structure (Zintl phase),-which expands not only in the direction of the quasibinary cut $Li(Au_xIn_{1-x})$ with $0 \le x \le 0.5$, but also into the directions of both higher and lower Li-concentrations.

1. Introduction

An important characteristic of intermetallic compounds from three elements is their homogeneity range in the corresponding phase diagram. Two cases have to be distinguished: compounds are called "real" ternary compounds in the definition of [1], when their homogeneity range does not extend to any of the binary end members. Otherwise, they are called "pseudoternary" phases and represent solid solutions of binary compounds with homogeneity ranges, expanding into the ternary isothermal phase diagram (concentration triangle). The three constituting elements are called "compound formers" when at least one "real" ternary compound exists, otherwise "compound nonformers". Up to now only empirical criteria are proposed for the prediction of "real" ternary phase formation in ternary systems. Therefore, the investigation of homogeneity ranges of ternary phases is crucial to elucidate the preconditions for the formation of "real" ternary phases.

Two "real" ternary compounds were recently found in the Li–Ag–In system and structurally characterized by X-ray diffraction on single crystals and powders: The first one is $LiAg_2In$ with a $MnCu_2Al$-type structure (*Fm*-3*m*, $a=6.5681(5)$ Å) and therefore called a Heusler phase [2], independent from the magnetic properties. The second one is $Li_{278}(In, Ag)_{154}$ with approximate composition $Li_{278}Ag_{40}In_{114}$, which crystallizes in a $n=6$ variant of a cubic *n x n x n* W-type superstructure with 432 atoms in the unit cell (*F*-43*m*, $a=20.089(2)$ Å) [3]. In addition to these two real ternary compounds, a wide homogeneity range of the pseudoternary Zintl phase $Li(Ag_xIn_{1-x})$ with $0 \le x \le 0.5$ is known with LiIn as the binary endpoint of this quasibinary cut [4–6]. The homogeneity region of this pseudoternary Zintl phase is considerably expanded into the lithium richer direction and also, but to a smaller extent, into the lithium poorer region [7]. In this contribution we report on an investigation of the structural analogy between the Li–Ag–In and the Li–Au–In system with respect to their interpretation as compound formers or nonformers, based on the existence of real or pseudoternary phases.

2. Experimental

The investigated samples were prepared from the following reactants: lithium (rod of 10 mm diameter, 99.9 at%, AlfaAesar), indium (ingots, 99.999 at%, ChemPur) and gold (foil of 0.5 mm thickness, 99.999 at%, AlfaAesar). Appropriate amounts were mixed according to the aimed stoichiometry of the product and filled into unalloyed iron crucibles in the glove box under dry argon atmosphere. These crucibles have been sealed by welding under dry argon atmosphere, placed into a preheated furnace (1100 °C) and heavily shaked to mix up the reactants properly. Note that the use of unalloyed iron is essential to avoid any unwanted alloy formation with material from the crucible in this temperature range. After 10 min the samples were rapidly cooled down to room temperature by removing the crucibles from the furnace into ambient conditions. The reaction product was powdered in an agate mortar. Single crystals of $LiAu_2In$ were screened using a light microscope with the sample protected against atmosphere under dried paraffin. An Xcalibur diffractometer from Oxford Diffraction, equipped with a

* Corresponding author.
E-mail address: helmut.ehrenberg@kit.edu (H. Ehrenberg).

0022-4596/$ - see front matter © 2011 Elsevier Inc. All rights reserved.
doi:10.1016/j.jssc.2011.03.020

Sapphire2 CCD detector and an ENHANCE X-ray source option, was used for single crystal X-ray diffraction (Mo-$K\alpha_1$, 7 φ-scans for intensity data collection).

X-ray powder diffraction patterns were collected on a STOE STADI P with Mo-$K\alpha_1$ radiation in Debye–Scherrer mode, using closed capillaries with diameters of 0.3 or 0.5 mm. The software package WinPlotr was used for Rietveld refinements [12].

The amount of Li-loss during sample preparation in hermetically closed crucibles can be estimated, based on previous studies with successive detailed chemical analyses of similar systems [4,5,8,9]. Accordingly, an alkaline loss between 0% and 0.7% versus the nominal composition can be expected.

3. Structure determination of $LiAu_2In$

All observed reflections from the single crystal XRD can be indexed, based on a face-centered cubic cell without any additional extinction rules (a=6.4982(8) Å). A combined empirical absorption correction with frame scaling was applied, using the *SCALE*3 *ABSPACK* command in CrysalisRed [10]. The structure has been solved by direct methods and refined using the SHELX-97 package program [11]. An initial parameter set was obtained from automatic interpretations of direct methods using SHELXS-97, and this structure model was further refined using SHELXL-97 until convergence was reached. The final parameters for the model with lowest R_1-value are summarized in Table 1, atomic coordinates and equivalent isotropic displacement parameters are presented in Table 2. One unit cell and the coordination polyhedra of $LiAu_2In$ are essentially the same like in the $LiAg_2In$ compound [2]. The final crystal structure was refined in the *Fm*-3*m* space group, a=6.4976(3) Å up to a Bragg R-factor=6.23% and RF-factor=5.22%, based on X-ray powder diffraction data . The experimental X-ray diffraction pattern, calculated profiles and their difference curve after Rietveld refinement are shown in Fig. 1. Note that the sample shows anisotropic peak broadening: reflections *h*00 appear broader than *hhh* reflections.

Table 1
Crystal data and structure refinement for $LiAu_2In$.

Empirical formula	$(Li_{0.87}In_{0.13})Au_2In$*
Formula weight	2121.49
Temperature	298(2) K
Wavelength	0.71073 Å
Crystal system, space group	cubic, *Fm*-3*m*
Unit cell dimensions	a=6.4982(8) Å
Volume	274.40(6) Å^3
Z, Calculated density	4, 12.483 g/cm^3
Absorption coefficient	115.740 mm^{-1}
F (0 0 0)	865
Theta range for data collection	5.44, 25.94°.
Index ranges	$-8<=h<=8$, $-7<=k<=7$, $-7<=l<=7$
Reflections collected/unique	348/26 [$R(int)$=0.09]
Refinement method	Full-matrix least-squares on F^2
Data/restraints/parameters	26/0/6
Goodness-of-fit on F^2	1.097
Final R indices [I > 2sigma(I)]	$R1$=0.0469, $wR2$=0.1012
Extinction coefficient	0.004(3)
Largest diff. peak and hole	−6.96 and 2.40 e Å^{-3}

* Note, that the refined Li-deficiency on the (4*b*)-site is most probably not due to a Li-loss but rather to a respective vice versa replacement of In and Au atoms by some Li atoms, thus not associated with a change of the overall composition. Such a mixed occupation cannot be distinguished from the here reported site occupation by X-ray diffraction data and, therefore, not considered as a structural degree of freedom. This here registered 13% admixture of In-atoms on the Li-site resembles the analog finding for the single crystal of $LiAg_2In$, but is approximately twice as high. An occupation of In on the Li-site of $LiAu_2In$ is not confirmed by X-ray powder diffraction.

Table 2
Atomic coordinates and equivalent isotropic displacement parameters for $LiAu_2In$.

Atom	Site	x/a	y/b	z/c	U (eq) (Å^2)
4 In	4*a*	0	0	0	0.042(2)
8 Au	8*c*	1/4	1/4	1/4	0.044(2)
3.46(6)Li+0.54In*	4*b*	1/2	1/2	1/2	0.04(1)

* Note, that the refined Li-deficiency on the (4*b*)-site is most probably not due to a Li-loss but rather to a respective vice versa replacement of In and Au atoms by some Li atoms, thus not associated with a change of the overall composition. Such a mixed occupation cannot be distinguished from the here reported site occupation by X-ray diffraction data and, therefore, not considered as a structural degree of freedom. This here registered 13% admixture of In-atoms on the Li-site resembles the analog finding for the single crystal of $LiAg_2In$, but is approximately twice as high. An occupation of In on the Li-site of $LiAu_2In$ is not confirmed by X-ray powder diffraction.

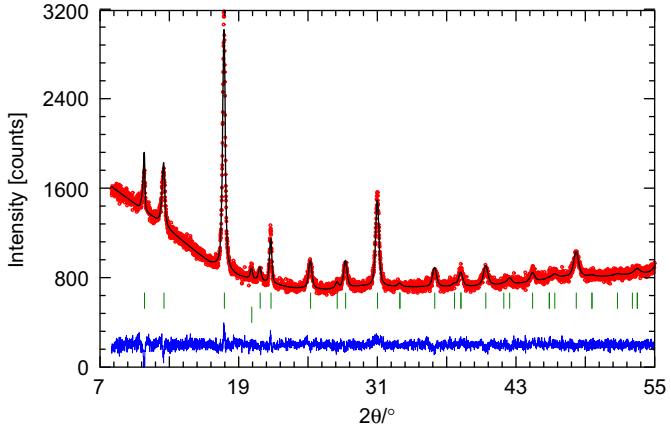

Fig. 1. Observed and calculated X-ray powder diffraction patterns together with their difference curve (bottom) for the $LiAu_2In$ compound. The one reflection in the lower line of reflection marks is the 200 reflection of a small Au impurity (less than 0.5% w/w).

Table 3
Rietveld refinement of the crystal structure of $Li_{0.65}Au_{0.05}In_{0.30}$.

Method	Full profile refinement of X-ray powder diffraction data
Structure type	$Li_{278}(Ag, In)_{154}$
Space group, Pearson symbol, Z	*F*-43*m*, *c*F432, Z=1
Lattice parameters	a=19.9970(2) Å
2θ range	$3.00<2\theta<49.99$
No. of fitted parameters	57
Halfwidth U, V, W, X (profile function no. 7)	0.00000, 0.00000, 0.008519, 0.425228

4. Structure determination of $Li_{280}Au_{22}In_{130}$ ($Li_{0.65}Au_{0.05}In_{0.30}$)

Four Li–Au–In alloys of the n=6 variant of a cubic $n\times n\times n$ W-type superstructure with a composition close to the known isostructural compound $Li_{278}Ag_{40}In_{114}$ have been prepared and structurally analyzed by X-ray powder diffraction: $Li_{0.65}Au_{0.05}In_{0.30}$, $Li_{0.65}Au_{0.07}In_{0.28}$, $Li_{0.65}Au_{0.10}In_{0.25}$, and $Li_{0.643}Au_{0.093}In_{0.264}$ (respectively, $Li_{280}Au_{22}In_{130}$, $Li_{281}Au_{30}In_{121}$, $Li_{280}Au_{43}In_{108}$, and $Li_{278}Au_{40}In_{114}$). The alloys $Li_{0.65}Au_{0.05}In_{0.30}$ and $Li_{0.65}Au_{0.07}In_{0.28}$ are homogeneous with a $Li_{278}(Ag, In)_{154}$ analog structure, while the alloys $Li_{0.65}Au_{0.10}In_{0.25}$ and $Li_{0.643}Au_{0.093}In_{0.274}$ are heterogeneous and contain small amounts of an additional Zintl phase. The structural details of the alloy $Li_{0.65}Au_{0.05}In_{0.30}$ are summarized in Tables 3 and 4, and the observed and calculated profiles are shown in Fig. 2. For

Table 4
Atomic parameters in the structures of the $Li_{280}Au_{22}In_{130}$ and $Li_{278}Ag_{40}In_{114}$ compounds.

Wyck. site	Atom	$Li_{280}Au_{22}In_{130}$ ($Li_{65}Au_5In_{30}$)				$Li_{278}Ag_{40}In_{114}$			
		x/*a*	*y*/*b*	*z*/*c*	Occupation	*x*/*a*	*y*/*b*	*z*/*c*	Occupation
24*f*	M1	0.3280	0	0	0.940-In, 0.060-Au	0.3329	0	0	1.000-In
16*e*	M2	0.9145	0.9145	0.9145	0.940-In, 0.060-Au	0.9156	0.9156	0.9156	1.000-In
48*h*	M3	0.1679	0.1679	0.0007	0.520-In, 0.480-Li	0.1661	0.1661	0.0039	0.544-In, 0.456-Li
48*h*	M4	0.0827	0.0827	0.2505	0.940-In, 0.060-Li	0.0819	0.0819	0.2518	0.753-In, 0.247-Li
16*e*	M5	0.3266	0.3266	0.3266	0.646-In, 0.354-Li	0.3312	0.3312	0.3312	0.765-In, 0.235-Li
16*e*	M6	0.6669	0.6669	0.6669	0.387-Li, 0.353-Au, 0.260-In	0.6658	0.6658	0.6658	1.000-Ag
24*g*	M7	0.5844	1/4	1/4	0.731-Li, 0.158-Au, 0.111-In	0.5888	1/4	1/4	0.539-Ag, 0.461-Li
4*c*	M8	1/4	1/4	1/4	0.748-Au, 0.252-In	1/4	1/4	1/4	0.820-Ag, 0.180-Li
16*e*	M9	0.5794	0.5794	0.5794	0.673-Li, 0.198-Au, 0.129-In	0.5834	0.5834	0.5834	0.571-Li, 0.429-Ag
4*a*	M10	0	0	0	0.941-Li, 0.042-Au, 0.017-In	0	0	0	0.800-Li, 0.200-Ag
48*h*	Li11	0.0833	0.0833	0.7500	1.000	0.0837	0.0837	0.7437	1.000
48*h*	Li12	0.1667	0.1667	0.5000	1.000	0.1681	0.1681	0.5029	1.000
24*g*	Li13	0.0833	1/4	1/4	1.000	0.0708	1/4	1/4	1.000
24*f*	Li14	0.1667	0	0	1.000	0.1708	0	0	1.000
16*e*	Li15	0.8333	0.8333	0.8333	1.000	0.8324	0.8324	0.8324	1.000
16*e*	Li16	0.0833	0.0833	0.0833	1.000	0.0778	0.0778	0.0778	1.000
16*e*	Li17	0.1667	0.1667	0.1667	1.000	0.1667	0.1667	0.1667	1.000
16*e*	Li18	0.4167	0.4167	0.4167	1.000	0.4094	0.4094	0.4094	1.000
4*b*	Li19	1/2	1/2	1/2	1.000	1/2	1/2	1/2	1.000
4*d*	Li20	3/4	3/4	3/4	1.000	3/4	3/4	3/4	1.000

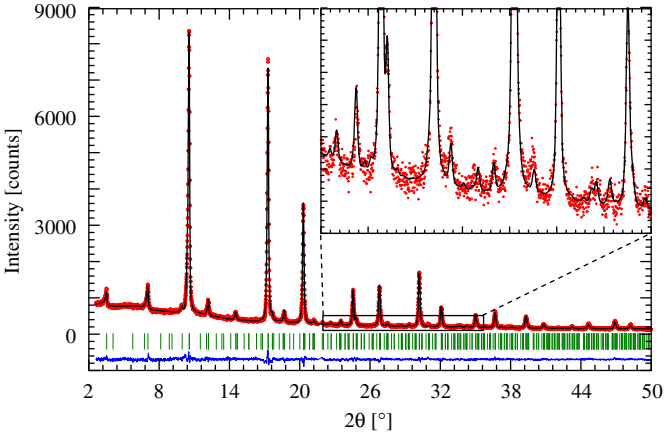

Fig. 2. Observed and calculated X-ray powder diffraction patterns together with their difference curve for $Li_{0.65}Au_{0.05}In_{0.30}$ as representative for the $n=6$ variant of a cubic $n \times n \times n$ W-type superstructure for the corresponding ternary Li–Au–In phase (one very tiny reflection of a nonidentified phase has been excluded). A zoom of a low-intensity region with some weak superstructure reflections is shown in the inset.

comparison Table 4 includes also the respective details of the isostructural $Li_{278}Ag_{40}In_{114}$ compound. From none of the Au-containing alloys an adequate single crystal with acceptable quality for X-ray or neutron structure analysis could be extracted in contrast to the Ag-containing alloy. Therefore, in Table 4 results from X-ray powder diffraction of $Li_{0.65}Au_{0.05}In_{0.30}$ are compared with results from a single crystal X-ray structure analysis of $Li_{278}Ag_{40}In_{114}$.

Note that in the case of the Au-containing alloy the discrimination between Au and In by X-ray diffraction is more reliable than the respective discrimination between Ag and In in case of the Ag containing alloy. Therefore reliable results about the occupancies on the Wyckoff sites can be deduced even from X-ray powder diffraction in the case of the Au-containing alloys with some limitations due to an under determination of the high number of structure parameters compared to the restricted information, caused by significant peak overlap in the powder diffraction pattern. However, two reasonable constraints reduce the ambiguity of distinct models with non-distinguishable calculated

Table 5
Atomic parameters for the different alloys of solid solution Zintl phases, based on space group *F*-43*m*.

Atom	Wyckoff site	Occupation	*x*/*a*	*y*/*b*	*z*/*c*
$Li_{0.56}Au_{0.22}In_{0.22}$					
Li1	4*a*	100%	0	0	0
Li2	4*b*	100%	1/4	1/4	1/4
M3	4*c*	Au–88(1)%, Li–12(1)%	1/2	1/2	1/2
M4	4*d*	In–88(1)%, Li–12(1)%	3/4	3/4	3/4
$Li_{0.560}Au_{0.095}In_{0.345}$					
Li1	4*a*	100%	0	0	0
Li2	4*b*	100%	1/4	1/4	1/4
M3	4*c*	Au–38(1)%, In–38(1)% Li–24%	1/2	1/2	1/2
In4	4*d*	100%	3/4	3/4	3/4
$Li_{0.46}Au_{0.27}In_{0.27}$					
M1	4*a*	Li–92(1)%, Au–8(1)%	0	0	0
M2	4*b*	Li–92(1)%, In–8(1)%	1/4	1/4	1/4
Au3	4*c*	100%	1/2	1/2	1/2
In4	4*d*	100%	3/4	3/4	3/4

diffraction patterns considerably: First, the same sets of 10 sites with an occupation of some heavy metals and other 10 sites, which are exclusively occupied with Li, are chosen in analogy to the Ag-containing compound, where a very reliable discrimination of Li and heavy metals could be concluded from single crystal diffraction data. The second constraint is the overall composition, determined by the ratio of the educts. In order to comply with these two constraints some In-sites require certain admixtures of Au and some Au-sites certain admixtures of In, beyond the structure model for the Ag-containing compound, where In and Ag could not be distinguished reliably by X-ray diffraction. Table 4 presents an appropriate structure model with a possible site-specific distribution of In and Au on the respective sites. This model cannot be confirmed unambiguously, but represents a local minimum in the residual difference between observed and calculated diffraction data. Note that the coordinates for the sites Li11–Li20 in Table 4, which are exclusively occupied by Li, were not refined for the Au-containing compound, but represent the idealized positions as derived from the underlying W-type structure, in contrast to the Ag-containing compound, where these coordinates were refined based on single crystal diffraction data.

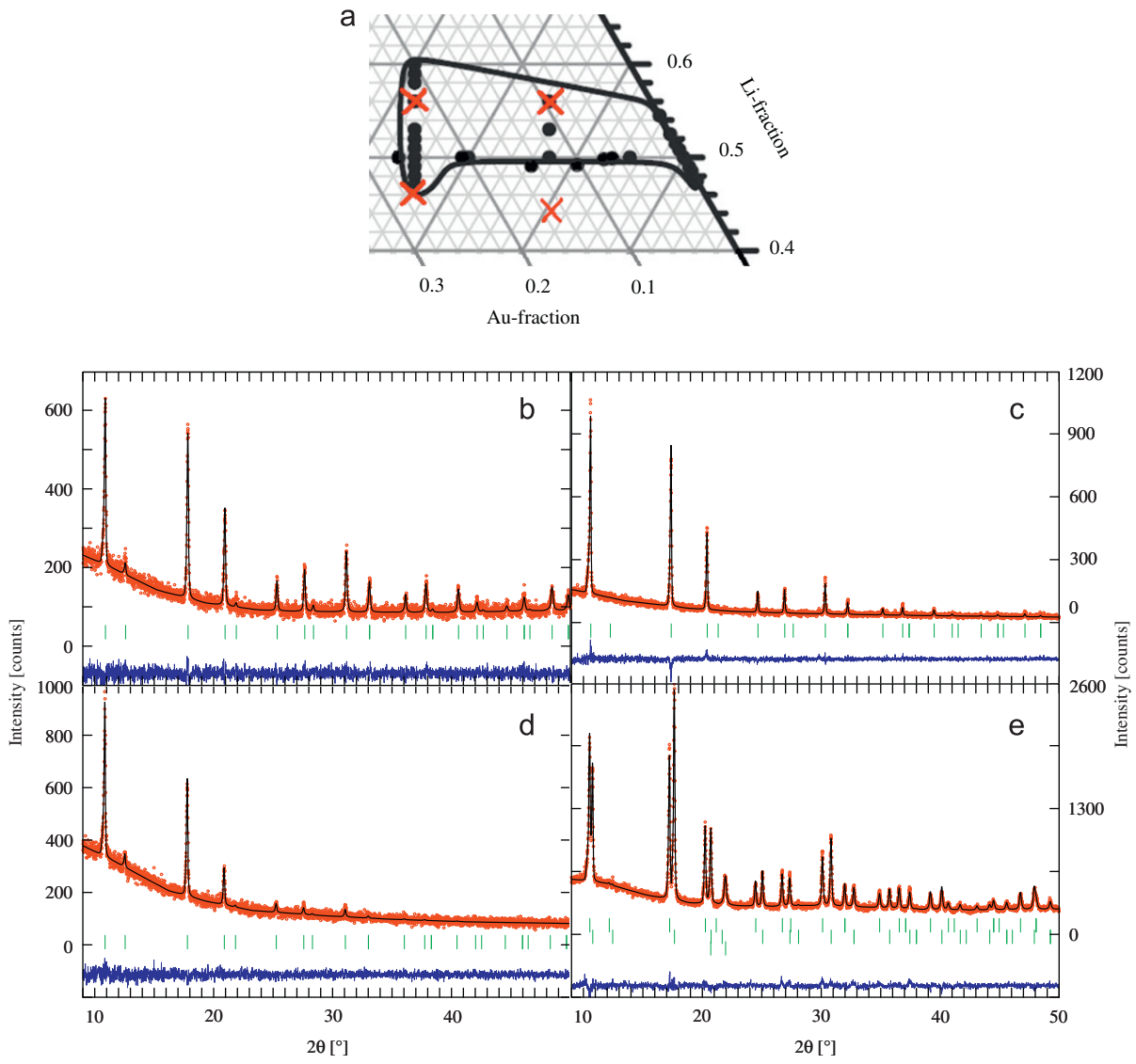

Fig. 3. (a) Alloys from the homogeneity range of the Zintl phase solid solutions in the Li–Ag–In system (circles) and in the Li–Au–In system (crosses). The observed and calculated diffraction patterns are shown together with their difference curve for $Li_{56}Au_{22}In_{22}$ (b), $Li_{56}Au_{9.5}In_{34.5}$ (c), $Li_{46}Au_{27}In_{27}$ (d) and $Li_{44}Au_{15.5}In_{40.5}$ (e).

Alloys with the composition $Li_{0.65}Au_{0.10}In_{0.25}$ and $Li_{0.643}Au_{0.093}In_{0.264}$ contain two phases. The major phase is $Li_{280}Au_{22}In_{130}$, the minor phase was identified as a solid solution Zintl phase with NaTl-type structure. The lattice constants of the Au-containing main phases were refined to $a=19.9233(4)$ Å (0.10 Au) and $a=19.864(1)$ Å (0.093 Au), respectively.

5. Determination of the homogeneity range of the solid solution Zintl phase

In the Li–Au–In system an expansion of the homogeneity range of the quasibinary cut $Li(Au_xIn_{1-x})$ with $0\le x\le 0.5$ as a solid solution of a pseudoternary Zintl phase into the Li-poorer and Li-richer regions was also expected like yet established in the Li–Ag–In–system [7]. Two alloys with the compositions $Li_{0.46}Au_{0.27}In_{0.27}$ and $Li_{0.56}Au_{0.22}In_{0.22}$ along the quasibinary cut $Li_x(Au_{0.5}In_{0.5})_{1-x}$ and two alloys outside this quasibinary cut with the compositions $Li_{0.440}Au_{0.155}In_{0.405}$ and $Li_{0.560}Au_{0.095}In_{0.345}$ were synthesized and analyzed by X-ray powder diffraction. Three of the synthesized alloys were single phases (see Fig. 3a–d) like in the corresponding Li–Ag–In system (see Fig. 3a), one was heterogeneous (see Fig. 3a and e). In the Au-containing phase the ordered alternative of the NaTl-type Zintl phases came out very clear, whereas in the Ag-system the discrimination between a statistical mixture of Ag and In on one site in the space group $Fd3m$ and an ordered occupation of Ag and In on distinct sites in the space group $F\text{-}43m$ was not very reliable due to the similarity of the X-ray scattering power of Ag and In. The lattice constants and some statistical data for the homogeneous Zintl phases are: $Li_{0.56}Au_{0.22}In_{0.22}$ ($a=6.4663(2)$ Å, Bragg R-factor=6.96%, RF-factor=6.41%), $Li_{0.560}Au_{0.095}In_{0.345}$ ($a=6.6386(2)$ Å, Bragg R-factor=10.5%, RF-factor=10.1%) and $Li_{0.46}Au_{0.27}In_{0.27}$ ($a=6.4857(5)$ Å, Bragg R-factor=7.21%, RF-factor=9.21%). The atomic parameters of these 3 homogeneous phases are given in Table 5.

The fourth alloy with the composition $Li_{0.440}Au_{0.155}In_{0.405}$ consists mainly of two phases, see Fig. 3(a and e): One is a partially ordered Zintl phase with composition $Li_{0.500}Au_{0.080}In_{0.420}$, deduced from the refined lattice parameter $a=6.6886(1)$ Å (Bragg R-factor=4.28%, RF-factor=4.86%) and the dependence of lattice parameter on composition for the quasibinary cut $Li_{0.5}(Au_xIn_{1-x})_{0.5}$ with $0\le x\le 0.5$ [5]. The other is an also partially ordered Heusler phase with the composition $Li_{0.365}Au_{0.250}In_{0.385}$ ($a=6.5356(1)$ Å,

Bragg *R*-factor = 5.75%, *RF*-factor = 5.38%). Note that the composition of this Heusler phase differs considerably from the composition of the above described $LiAu_2In$-Heusler phase, i.e. the ratio of the heavy metals Au/In $\gg 1$ is converted to Au/In $\ll 1$. The difference between these two Heusler phases is most pronounced in the different occupations of the 8*c* Wyckoff site: in $LiAu_2In$ this site is exclusively occupied by Au and in $Li_{0.365}Au_{0.250}In_{0.385}$ by a statistical mixture of 77% In and 23% Li. Therefore, instead of one broad homogeneity range including these both Heusler phases, the existence of a second real ternary Heusler phase region might be probable, which could even include the composition $LiAuIn_2$. The molar ratios of Zintl to Heusler phases in the alloy with the composition $Li_{0.440}Au_{0.155}In_{0.405}$ came out in very good agreement as 56:44 (calculated from composition) and 58:42 (from Rietveld refinement), respectively. Note that the small contribution from a third phase, treated by profile matching mode and probably comes from the crucible, see Fig. 3(e), was not included in the determination of these phase ratios.

6. Summary

Three ternary phases were established in the Li–Au–In system. The phase with an $n=6$ variant of a cubic $n \times n \times n$ W-type superstructure and the Heusler phase are real ternary phases, while the ordered Zintl phase with NaTl-type structure is a pseudoternary phase. The existence of these three ternary phases and there respective homogeneity ranges are in full agreement with those in the Li–Ag–In system. Especially, the pseudoternary Zintl phase reveals also a similar expansion of its homogeneity range into the lithium richer and lithium poorer region.

Acknowledgement

Financial support from the *Deutsche Forschungsgemeinschaft* (DFG), the Ministry of Education and Science of Ukraine (M/206–2009) and the *Bundesministerium für Bildung und Forschung* (WTZ UKR 08/024) is gratefully acknowledged.

References

[1] P. Villars, K. Brandenburg, M. Berndt, S. LeClair, A. Jackson, Y.-H. Pao, B. Igelnik, M. Oxley, B. Bakshi, P. Chen, S. Iwata, J. Alloys Compd. 317–318 (2001) 26–38.
[2] V. Pavlyuk, G. Dmytriv, I. Chumak, H. Ehrenberg, H. Pauly, J. Solid State Chem. 178 (2005) 3303–3307.
[3] V.V. Pavlyuk, G.S. Dmytriv, I.I. Tarasiuk, H. Pauly, H. Ehrenberg, Intermetallics 15 (2007) 1409–1415.
[4] H. Pauly, A. Weiss, H. Witte, Z. Metallk. 59 (1968) 47–58.
[5] H. Pauly, A. Weiss, H. Witte, Z. Metallk. 59 (1968) 554–558.
[6] G Effenberg, F Aldinger, O Bodak, VV Pavlyuk (Eds.), Ternary alloys (+binary +quaternary systems. Evaluated constitutional data, phase diagrams, crystal structures and applications of lithium alloy systems), vol. 14, VCH, D-69496 Weinheim, Germany, 1995, p. 458.
[7] G.S. Dmytriv, H. Pauly, H. Ehrenberg, V.V. Pavlyuk, E. Vollmar, J. Solid State Chem. 178 (2005) 2825–2831.
[8] H. Pauly, Diploma Thesis, Faculty of Chemistry, Darmstadt University of Technology, 1963.
[9] H. Pauly, Ph.D. Thesis, Faculty of Chemistry, Darmstadt University of Technology, 1966.
[10] CrysalisRed, CCD, data reduction GUI. version 1.171.26, Oxford Diffraction Poland Sp, 2005.
[11] G.M. Sheldrick, SHELXL-97. Program for Crystal Structure Refinement, University of Göttingen, Germany, 1997.
[12] T. Roisnel, J. Rodriguez-Carvajal, Mater. Sci. Forum 378–381 (2001) 118–123.